

## Direct Detection EELS at High Energy: Elemental Mapping and EXELFS

James L. Hart<sup>1</sup>, Andrew C. Lang<sup>1</sup>, Rebecca B. Cummings<sup>2</sup>, Ian MacLaren<sup>2</sup>, Mitra L. Taheri<sup>1\*</sup>

1. Department of Materials Science & Engineering, Drexel University, Philadelphia, PA 19104, USA

2. School of Physics and Astronomy, University of Glasgow, Glasgow G12 8QQ, UK

\*Corresponding author: mtaheri@coe.drexel.edu

Electron energy-loss spectroscopy (EELS) is a powerful technique for nanoscale elemental mapping and determination of chemistry, such as oxidation state. One limitation, however, is that the acquisition of high quality high energy edges beyond ~3 keV is difficult. This restriction is problematic for both elemental mapping and oxidation state determination of certain elements. Moreover, extended energy loss fine structure (EXELFS) analysis – which yields an element's radial distribution function (RDF) – generally requires measurement of high energy *K*-edges, making RDF determination challenging with conventional EELS. Recently, progress has been made in optimizing the optical coupling to allow experimental observation of high energy edges out to 10 keV [1,2], but signal to noise ratio (SNR) remains a limiting factor. We have previously shown that spectral SNR can be improved through the use of direct detection (DD) technology and electron counting [3]. Here, we investigate the use of DD EELS on high energy edges; we demonstrate improved elemental mapping capabilities and show that EXELFS on a high energy *K*-edge can provide accurate RDF determination within the TEM.

We use a Gatan K2 IS direct detection camera operated in electron counting mode with a Gatan GIF Quantum. The spectrometer also has a Gatan US1000FTXP, allowing a direct comparison between DD and conventional EELS. The DD sensor was operated at 0.5 eV/channel dispersion, and the conventional sensor at 1 eV/channel, with a ~2 keV field of view obtained in both cases. The GIF is mounted on a JEOL2100F microscope with a Schottky emitter, operated at 200 kV accelerating voltage. A custom camera length was used to provide a collection angle of ~60 mrad for 5 keV energy loss and good transfer into the spectrometer to well beyond this energy loss.

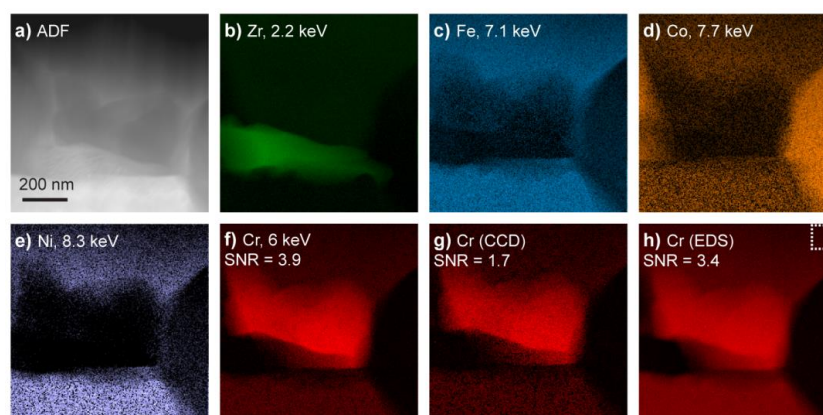
Figure 1a-f shows DD EELS mapping of an annealed ZrCrFeCoNi high entropy alloy sample, with the maps extracted from the transition metal *K*-edges (2-8 keV). To cover this large energy field of view, multiple spectrum images were taken. For comparison, we show a conventional EELS map of Cr (Fig. 1g) an EDS map (Fig. 1h) collected with an Oxford X-Max<sup>N</sup> 80T EDS system with an 80 mm<sup>2</sup> SSD. For all maps, a 60 ms pixel dwell time was used. We quantify the Cr *K*-edge map SNR and show that at this energy and sample thickness (~1 MFP), DD EELS provides the highest SNR, with the SNR for DD EELS, EDS, and conventional EELS being 3.9, 3.4, and 1.7, respectively (see figure caption for details). At higher energies, EDS provides the highest SNR. We anticipate that for thinner samples, e.g. for the study of nanoparticles and 2D materials, DD EELS will provide far greater SNR than the 80 mm<sup>2</sup> SSD EDS system.

Figure 2 shows EXELFS on the Ti *K*-edge from a pure Ti sample. The data was collected in conventional TEM (diffraction) mode over an area of 1 μm<sup>2</sup>. The beam current was roughly 4 nA, and the total acquisition time was 600 s. Figure 2a shows the deconvolved (sample thickness = 0.5 MFP) DD EELS data, and Fig. 2b shows  $\chi(k)$ , with the conversion to *k*-space performed within the Demeter software package [4]. Impressively, clear signal oscillations are observed out to 10 Å<sup>-1</sup>. For comparison, a conventional EELS dataset recorded on a CCD is shown in Fig. 2b, with the arrows indicating the

decreased SNR of conventional EELS. Figure 2c shows the EXELFS signal converted to real space from the DD EELS data, along with the theoretical RDF for unstrained HCP Ti. The high SNR in Fig. 2b and the good agreement between experiment and theory shown in Fig. 2c demonstrate that EXELFS is a practical technique for RDF determination within the TEM. In addition to the data included herein, we will discuss ongoing efforts to apply EXELFS to various EELS experiments where changes in RDF are driven by *in situ* annealing [5].

#### References:

- [1] A. J. Craven, H. Sawada, S. McFadzean and I. MacLaren, *Ultramicroscopy* **180** (2017), p. 66.  
 [2] I. Maclaren, K. J. Annand, C. Black, A. J. Craven., *Microscopy* **67** [S1] (2018), p. i78  
 [3] J.L. Hart *et al.*, *Scientific Reports* **7** (2017), article number 8243  
 [4] B. Ravel and M. Newville, *Journal of Synchrotron Radiation* **12** (2005), p. 537-541  
 [5] JLH, ACL, and MLT acknowledge funding from NSF MRI grant number 1429661. RBC acknowledges funding from the EPSRC for her studentship.



**Figure 1.** a) STEM-ADF image of a ZrNiFeCoCr sample after annealing and secondary phase formation. b-f) DD EELS elemental maps. g) and h) Conventional EELS and EDS maps, respectively, of the Cr *K*-edge signal for comparison with the DD EELS map shown in (f). The Cr map SNR was determined for f-h within the area marked in the upper right hand corner of (h). Within this area of constant Cr concentration, the signal was taken as the average Cr edge intensity, and the noise was taken as the edge intensity standard deviation.

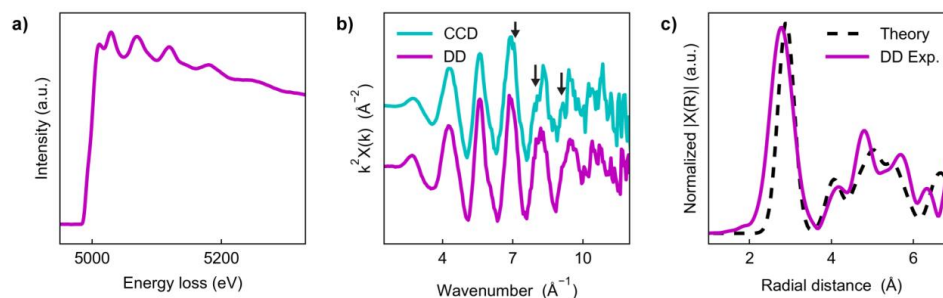


**Figure 2.** a) Ti *K*-edge spectra of a pure Ti sample. b) EXELFS signal in *k*-space for spectra collected with conventional and DD EELS. Arrows indicate increased noise in the conventional EELS data. c) Comparison of the Fourier transform of  $\chi(k)$  obtained with DD EELS and the theoretical RDF of Ti given its HCP crystal structure, assuming no strain or defects.